The effects of pressure on drawing polyoxymethylene: 2. Drawn fibre properties and structure

Tamikuni Komatsu, Sachio Enoki and Atsushi Aoshima
Technical Research Laboratory of Asahi Chemical Industry Co. Ltd, 2-1 Samejima, Fuji, Sizuoka 416, Japan
(Received 24 April 1989; revised 6 June 1990; accepted 14 June 1990)

Superdrawn polyoxymethylene fibres produced by pressurized drawing are dense and transparent, and have good mechanical properties. Maximum tensile modulus and strength and apparent density were found to be 58 GPa, 2.0 GPa and 1.45 g cm^{-3}, respectively. A study was made of the effects of pressure on the mechanical properties and structural characteristics of drawn fibres. The relationship between these parameters is discussed.

(Keywords: polyoxymethylene; pressure effect; structure; mechanical properties; drawn fibres)

INTRODUCTION

When a crystalline polymer with a lamellar structure is fully extended by mechanical force, the drawn fibres show considerably improved mechanical properties, such as with respect to tensile modulus and tensile strength along the fibre axis.

Polyoxymethylene (POM), an engineering plastic called polyacetal, is a crystalline polymer, and the theoretical Young's modulus along its chain axis has been shown to be 90 to 150 GPa[1,2]. High-modulus and high-strength oriented POM has been made in various ways, such as tensile drawing[3–6], hydrostatic extrusion[7–9] and tensile drawing under microwave heating[10–16]. Its mechanical properties and structure have also been extensively studied. A series of studies[10–16] on large-diameter POM fibres produced by microwave heating/drawing were recently reported by Nakagawa *et al.* However, all the highly oriented POM had conspicuous fibrils and many structural defects such as voids. In ropes, cables and tension members for optical fibres, the fibrils would cause fluff and wear by friction, and the voids would lead to buckling of the fibres and decrease in strength in proportion to their number. The structures of oriented fibres should be carefully studied to understand their mechanical properties.

A pressurized drawing process for preparing superdrawn POM fibres was recently devised and the effects of pressure on the mechanical properties and structural characteristics of superdrawn POM were examined. The relationship between these parameters was also determined.

EXPERIMENTAL

Sample preparation

A tube with an outer diameter of 3.2 mm and inner diameter of 1.0 mm was prepared by melt extrusion of an acetal homopolymer 'Tenac 3010' (Asahi Chemical Industry Co. Ltd; number-average molecular weight M_n, 63 000; apparent density, 1.42 g cm^{-3}; softening point, 174°C; melting point, 179°C). The tube was continuously two-step drawn by pressurized drawing to obtain rod-like drawn fibres (pressurized drawn fibres), under the following conditions:

(i) First step—first pressure vessel length, 2 m; feed speed, 0.1 m min^{-1}; take-up speed, 0.8 m min^{-1}; draw ratio, 8; drawing temperature, 145°C; pressure, 50 kg cm^{-2}.

(ii) Second step—second pressure vessel length, 12 m; feed speed, 0.8 m min^{-1}; take-up speed, 3.4 m min^{-1} maximum; draw ratio, 34 maximum; temperature, 165°C; pressure, 400 kg cm^{-2}.

Silicone oil (Toray Co. Ltd, silicone oil WF 30) was used as the pressurizing and heating medium. The fibres thus obtained were washed several times in fresh Freon-113 by extraction to remove silicone oil and then dried at room temperature. Silicon from the silicone oil contained in the fibres was analysed with a fluorescent X-ray spectrometer and found to be negligibly small, below the limit of detection of 2–3 ppm, as in the case of the undrawn tube. For comparison, in silicone oil and heated dry air, conventional drawing was carried out under the same conditions as for pressurized drawing except for a gauge pressure of 0 kg cm^{-2}. The hollow fibres obtained were washed out in the same manner as above (conventional drawn fibres).

Measurements

Tensile modulus and strength along the fibre axis were measured at room temperature on an Instron tensile testing machine according to JIS K7113 (1981). The modulus was determined from the slopes of the stress–strain curves at a strain of 0.2–0.3% using an extensometer. Sample gauge length was 150 mm, crosshead speed, 5 mm min^{-1}, and mark distance for strain measurement, 50 mm. Tensile strength was measured using two stainless reel chucks of 160 mm diameter. These provided a groove along the circumference of the reel to wind the sample and a chuck to fix the sample end. When the

0032-3861/91/111988-06

sample was tensile-tested using the reel chucks, cracks often occurred in the sample on the reel so that strength fluctuated greatly. This was avoided in the following way. The groove was covered with a rubber sheet 1 mm thick. The sample was wound twice on each reel, fixed on the chucks, and tensile-tested. Most of the samples were fractured at the centre of their sample length without cracking and fluctuation in strength could be minimized. The distance between the centres of the reels was 200 mm and the crosshead speed was 100 mm min^{-1}. Measurement was carried out five times and the results averaged. Fluctuation in strength was within about $\pm 2\%$.

The calculated draw ratios (λ) and apparent ratios (λ_{app}) were determined from the ratio of the sample weight per unit length and ratio of the cross-sectional area of the sample before and after drawing. The cross-sectional areas of the sample for calculation of the tensile modulus, strength and apparent draw ratio were determined by two methods. One was based on sample diameter. The outer diameter was measured with a micrometer and the inner one was found from a photograph of the cross-section. The modulus, strength and apparent draw ratio were designated E_{app}, σ_{app} and λ_{app}, respectively. The other method was based on sample weight per unit length and density (ρ_{cal}), the values of which were put at E_{cal} and σ_{cal}, respectively. The apparent density (ρ_{app}) was calculated from sample weight per unit length and diameter of the sample, and was also measured using aqueous potassium carbonate as the density medium within 30 min at 23°C according to JIS K7112 (1980). The values were equal within $\pm 0.2\%$ by both methods.

The density (ρ_{cal}) was determined from crystallinity as follows:

$$\rho_{cal} = \rho_c x_c + \rho_a (1 - x_c) \quad (1)$$

Crystal density ρ_c and amorphous density ρ_a were set[17] at 1.49 g cm^{-3} and 1.22 g cm^{-3}, respectively. Crystallinity x_c in equation (1) was determined by the n.m.r. method developed by Veeman *et al.*[18]. The relaxation spectrum of the drawm POM was observed by cross-polarization/ magic angle spinning using a high-resolution n.m.r. spectrometer (JEOL, FX-200). Crystallinity was also measured using a wide-angle X-ray diffractometer (WAXD) and differential scanning calorimetry (d.s.c.).

Crystallinity x_c was determined by WAXD with a fibre specimen holder by diffractometry (Shimazu Seisakusho Co., XD-3A) as follows. The sample was rotated at a speed of 57 rev min^{-1}. Nickel-filtered Cu Kα ($\lambda = 1.542$ Å) radiation through a pinhole collimator was used as the incident X-ray source, with a pinhole slit system, a position-sensitive proportional counter (PSPC) for detecting the diffracted beam and graphite monochromator. The diffraction profile was obtained by the $\theta - 2\theta$ continuous scanning method using an X-ray counter. The raw profile thus obtained was corrected for Lorenz factor:

$$L_p = [1 + \cos^2(2\theta')\cos^2(2\theta)]/(1 + \cos^2\theta')(\sin^2\theta \cos\theta)$$

where θ and θ' are the Bragg angles of the sample and monochromator, respectively. This was followed by elimination of the background and peak separation of the profile from the crystal and amorphous parts on a computer. For this elimination, the exponential function was used as background. Peak separation was carried out by curve fitting using a Gaussian distribution as the diffraction peak. Crystallinity x_c was calculated from $X_c = S_c/S_{all}$, where S_c is the area of the crystal part in the profile and S_{all} is the entire area of the profile.

Crystallinity x_c was determined by d.s.c. from the heat of fusion calibrated with indium. Sample weight was 3.0 mg, and the heating rate was 8°C min^{-1}. The heat of fusion of POM crystal was set[19] at 75.3 cal g^{-1}.

A WAXD photograph was taken with a Laue camera. The crystal orientation factor f_c was determined by an azimuthal scan of (100) reflection from $-90°$ to $+90°$ at a scanning speed of 4 deg min^{-1}. Nickel-filtered Cu Kα ($\lambda = 1.542$ Å) radiation served as the incident X-ray source. Factor f_c was calculated from the half-width (H) of the profile as:

$$f_c = (180\text{-}H)/180$$

Dependence of the melting point on heating rate was measured using a differential scanning calorimeter (Perkin–Elmer, DSC-2). Sample weight was 2.0 mg and the standard material was indium. Pore size was measured with an Hg porosimeter. Fibre structure was observed by a scanning electron microscope (Hitachi-Seisakusho Co., S-430). A small-angle X-ray scattering (SAXS) photograph was taken with a Laue camera (Shimazu Seisakusho Co., VD-2).

RESULTS AND DISCUSSION

Pressure effects on tensile properties

Figure 1 shows the tensile modulus vs. draw ratio for fibres prepared by pressurized and conventional drawing. The modulus of the pressurized fibres increased linearly up to $\lambda = 24$, slowly increased above it, and reached a maximum 58 GPa at $\lambda = 34$ ($E_{app} = 53$ GPa, $\lambda_{app} = 31$). The modulus of the conventional fibres increased with λ, but was less than that of the pressurized fibres at each λ; the modulus was 50 GPa at $\lambda = 29$ as a maximum value ($E_{app} = 40$ GPa, $\lambda_{app} = 22$).

Figure 2 shows the relationship between apparent tensile modulus at a constant λ of 22 and applied pressure. Modulus increased slowly with pressure, thus indicating that pressure could possibly lead to structural differences.

Figure 3 shows tensile strength vs. draw ratio. This shows a curve having a maximum value of the draw ratio. The strength σ_{app} of the pressurized fibres was higher than that of the conventional fibres at equal draw ratios. The σ_{app} value of the pressurized fibres increased linearly to $\lambda_{app} = 22$, reaching 2.0 GPa as a maximum, and decreasing above it. The conventional fibres increased linearly to $\lambda_{app} = 15$, slowly increased in the range $15 \leqslant \lambda_{app} \leqslant 18$, reached 1.4 GPa as a maximum, and decreased above $\lambda_{app} = 18$ ($\sigma_{cal} = 1.5$ GPa, $\lambda = 20$).

The strength of a superdrawn POM fibre has been reported as 2.5 GPa[3] for a zone drawn fibre ($\lambda = 15$), 1.7 GPa[4] for a two-step drawn fibre ($\lambda = 20$) and 1.7 GPa[10] for a large-diameter fibre prepared by microwave heating/drawing ($\lambda = 28$). The diameter and apparent strength (σ_{app}) of the fibre prepared by microwave drawing were calculated as 0.58 mm and 1.5 GPa from the void ratio of 16% in ref. 10, respectively. Griffith *et al.*[20] found the strength of a glass fibre to decrease rapidly with increase in diameter, and explained this as due to surface defects. Smook *et al.*[21] studied the fracture process of ultra-high-strength polyethylene (PE) fibres

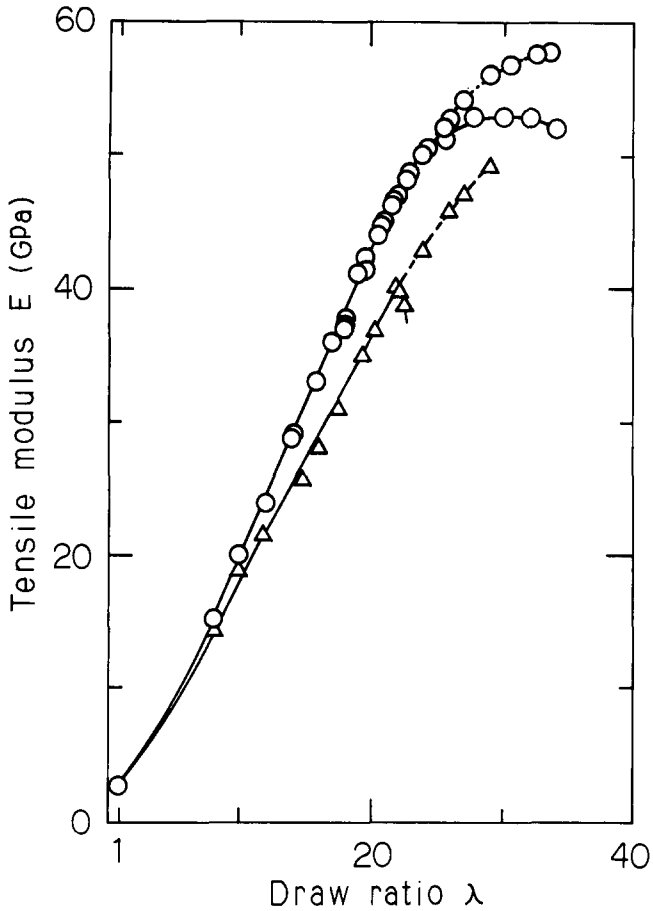

Figure 1 Tensile modulus vs. draw ratio for drawn POM fibres: (○) pressurized drawn fibre; (△) conventional drawn fibre. The full and broken curves indicate E_{app} vs. λ_{app} and E_{cal} vs. λ, respectively

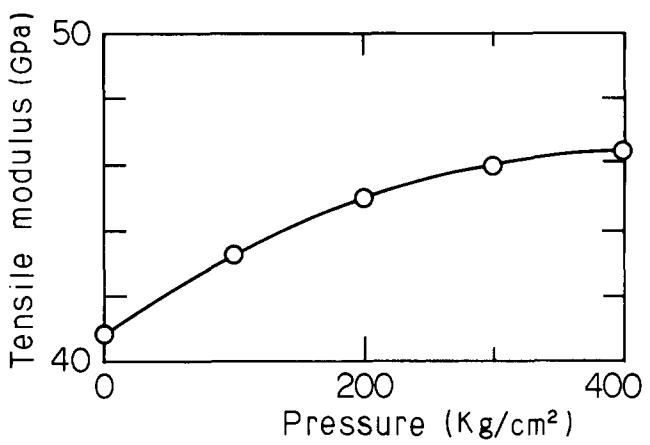

Figure 2 Tensile modulus vs. pressure of the POM fibres ($\lambda = 22$)

produced by gel-spinning/drawing and obtained the same results as Griffith. The high strength of 2.0 GPa for pressurized drawn fibres (diameter 0.66 mm) results from a structure without voids.

Effects of pressure on fibre structure

Pressurized drawn fibres were transparent up to $\lambda_{app} = 22$, translucent at $23 \leqslant \lambda_{app} \leqslant 24$, opaline at $\lambda_{app} =$ 25–26 and white above $\lambda_{app} = 26$. The conventional fibres were opaline up to $\lambda_{app} = 10$, and white above it.

The intact surface of the drawn fibres ($\lambda = 22$) is shown in *Figure 4*. The pressurized drawn fibre was free of voids and possessed a conspicuously fibrillar structure. The conventional fibre had voids appearing as a ladder connecting fibrils along the fibre axis. The SAXS patterns of the drawn fibres ($\lambda = 21$) could also be seen. The pressurized fibre had no equatorial scattering, while the conventional one showed strong equatorial streak scattering indicating the presence of voids. Pore size was measured with an Hg porosimeter. No pores could be found in the pressurized fibre, but micropores of 100–1000 Å in size were observed in the conventional fibre in addition to the macrovoids shown in *Figure 4b*.

Effects of pressure on density

Figure 5 shows apparent density vs. draw ratio for drawn fibres. The density of the pressurized fibres increased with λ, reaching 1.45 g cm^{-3} maximum at $\lambda_{app} = 22$ and decreasing slowly to 1.42 g cm^{-3} as undrawn POM at $\lambda_{app} = 26$. In contrast, the conventional fibres slowly decreased with λ to $\lambda_{app} = 18$ and rapidly above it. The decrease in density was due to voids generated during the drawing process. The void ratio was determined using:

$$f_v = (1 - \rho_{app}/\rho_{cal}) \times 100\% \quad (2)$$

Density ρ_{cal} was determined using equation (1). *Figure 6* shows the void ratio f_v vs. draw ratio. Changes in the void ratio in *Figure 6* and in apparent strength in *Figure 3* were related with each other. In the case of pressurized fibres, void generation was low up to $\lambda_{app} = 22$–24 where strength increased linearly. Above $\lambda_{app} = 26$, the strength

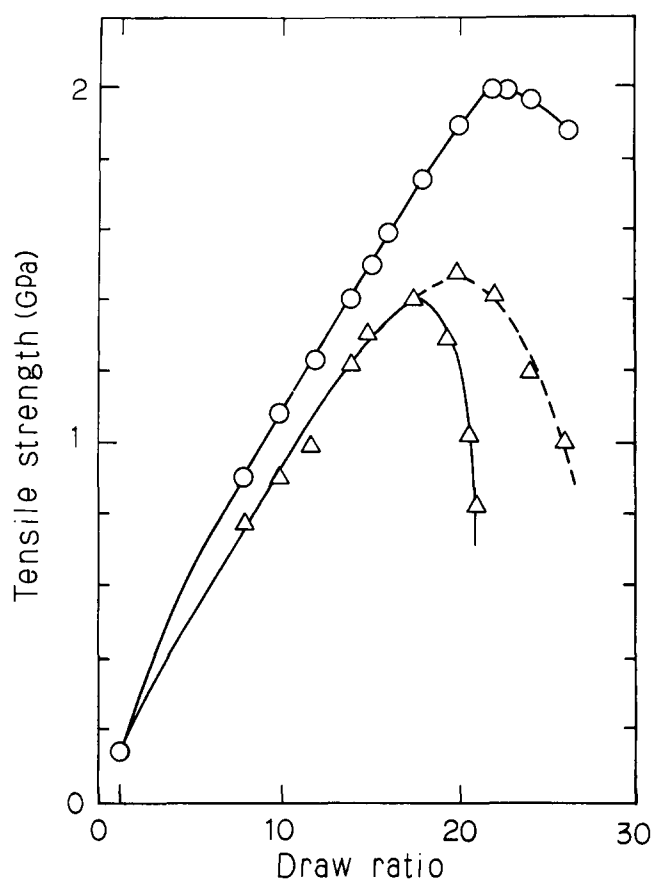

Figure 3 Tensile strength vs. draw ratio for drawm POM fibres: (○) pressurized drawn fibre; (△) conventional drawn fibre. The full and broken curves indicate σ_{app} vs. λ_{app} and σ_{cal} vs. λ, respectively

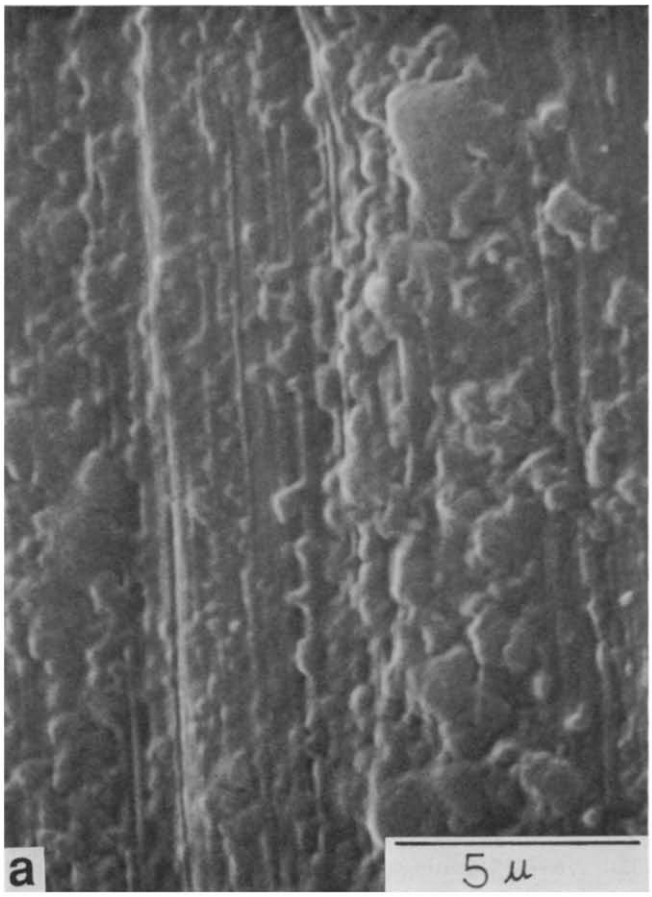

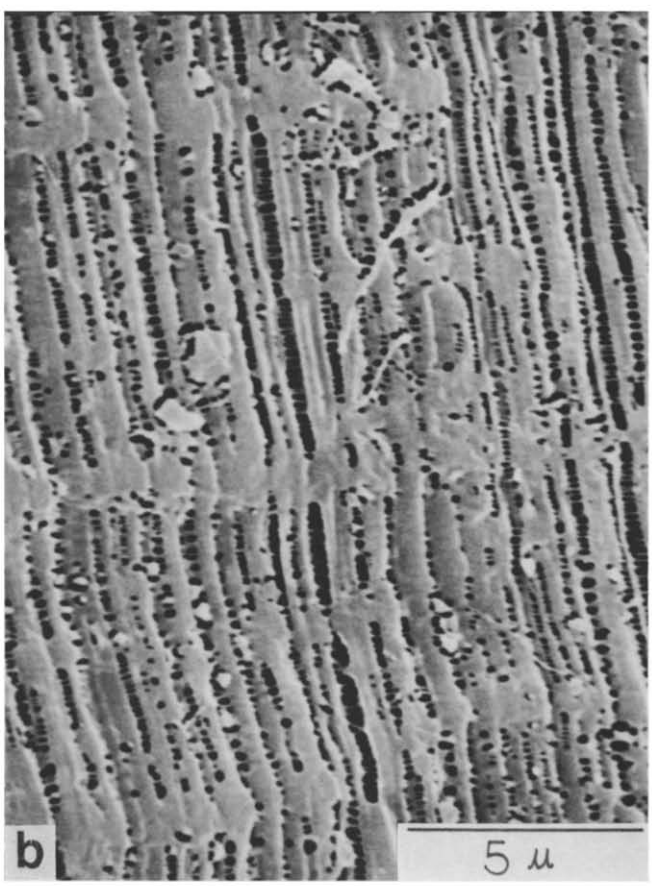

Figure 4 SEM micrographs of the surface of drawn POM fibres: (a) pressurized drawn fibre ($E_{cal}=44$ GPa, $\lambda=22$); (b) conventional drawn fibre ($E_{cal}=35$ GPa, $\lambda=22$)

decreased slightly. In the conventional fibres, strength increased linearly up to $\lambda_{app}=18$ where void generation was slight, but above this value the strength decreased rapidly. The decrease in strength is thus the result of void generation. The high strength of the pressurized fibres was due to dense structure being maintained even at high

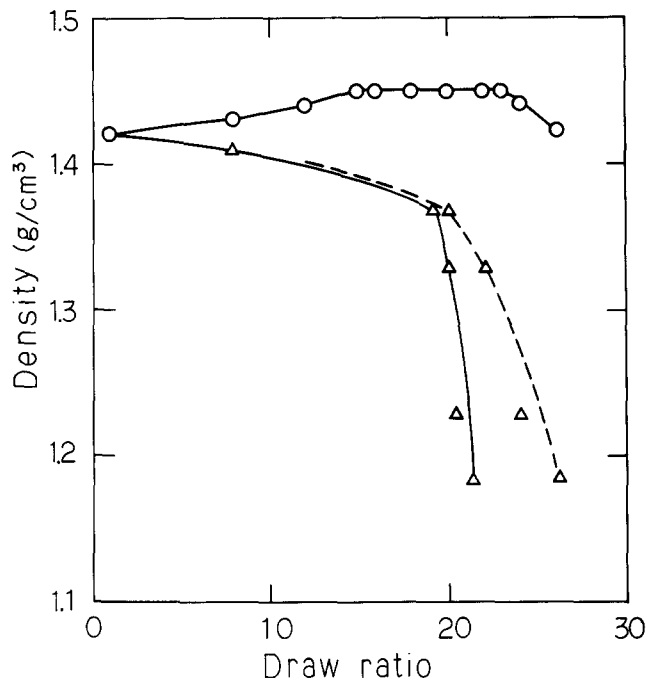

Figure 5 Apparent density vs. draw ratio for drawn POM fibres: (○) pressurized drawn fibre; (△) conventional drawn fibre. The full and broken curves indicate the apparent draw ratio and calculated one as abscissa, respectively

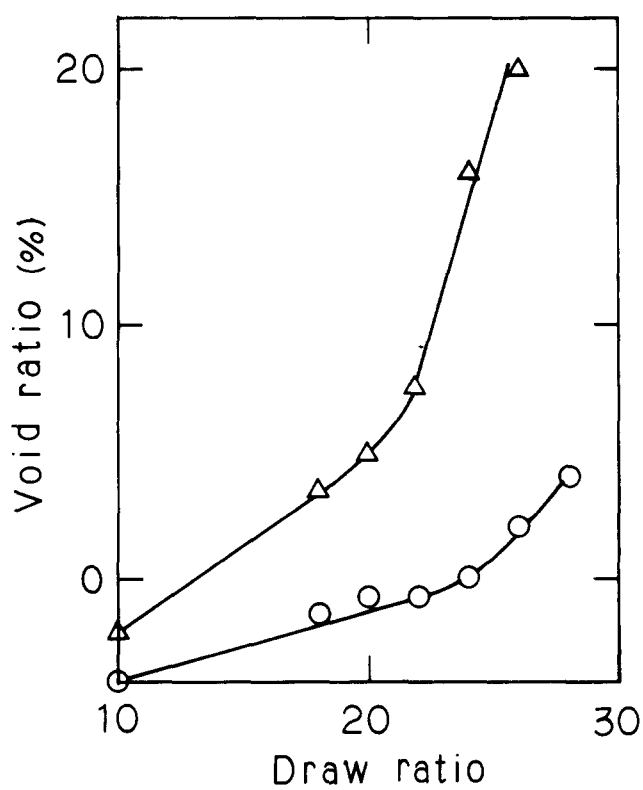

Figure 6 Void ratio f_v vs. draw ratio λ for drawn fibres: (○) pressurized drawn fibre; (△) conventional drawn fibre

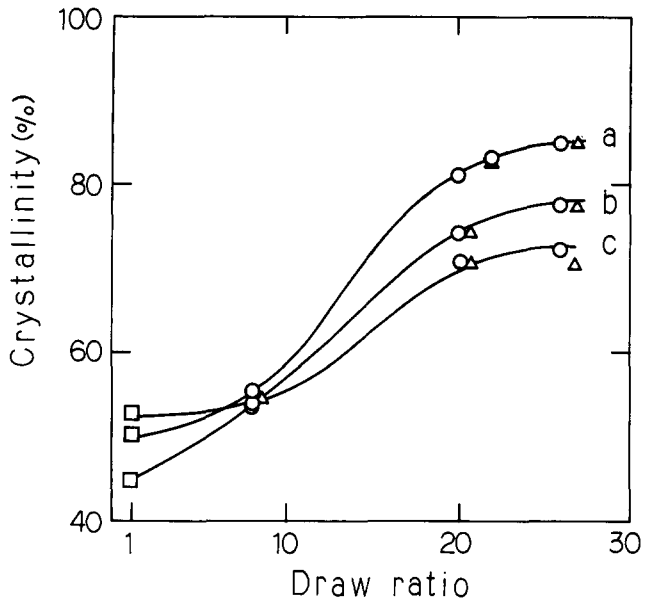

Figure 7 Crystallinity x_c vs. draw ratio λ for drawn POM fibres measured by several methods: (○) pressurized drawn fibre; (△) conventional drawn fibre; (a) n.m.r. method, (b) d.s.c. method, (c) X-ray method

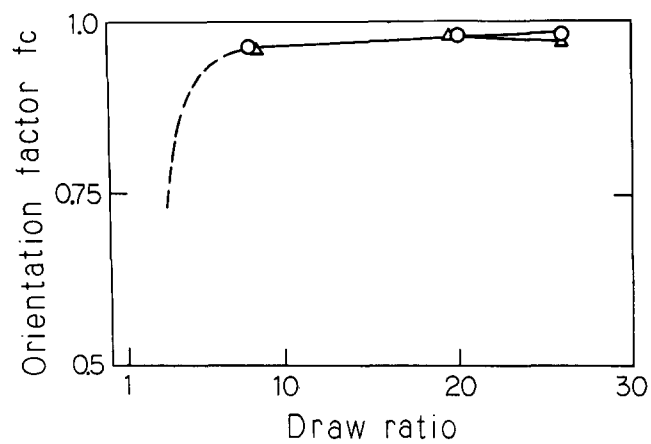

Figure 8 Crystalline orientation factor f_c vs. draw ratio λ for drawn POM fibres: (○) pressurized drawn fibre; (△) conventional drawn fibre

draw ratios where conventional drawing remarkably generates voids.

Crystallinity

Figure 7 shows the crystallinity x_c vs. draw ratio. The value of x_c increased with λ and was essentially the same for both fibres at a given draw ratio. Values for this parameter differed according to the mode of measurement. It increased rapidly to $\lambda=20$, and slowly above this value as shown by all modes.

Crystal orientation

WAXD photographs of drawn fibres ($\lambda=22$) were compared. The equatorial diffraction spot on the (1 0 0) plane of the pressurized fibre was slightly narrower than for the conventional fibre. A higher degree of orientation of the pressurized fibre thus appears possible. *Figure 8* shows the crystal orientation factor f_c vs. draw ratio. For both fibres f_c was almost the same below $\lambda=20$, but different above it. For the pressurized fibre it continued to increase slowly to $\lambda=26$, while for the conventional fibre it decreased above $\lambda=20$ in spite of increase in x_c. The decrease in f_c above $\lambda=20$ was probably due to rapid void generation.

Effects of structural factors on mechanical properties

Figures 1, 3, 7 and *8* indicate the following possibilities. The calculated tensile moduli of both fibres increased with x_c, but that of the pressurized fibre was higher than the conventional fibre in spite of the same x_c. The reason for this is not clear but may possibly be related to void structures characteristically observed in the conventional fibres, since the ladder in the vertical direction to the fibre axis did not contribute to tensile modulus. Strength increased with x_c when the number of voids was small. However, the rapid decrease in strength in the case of many voids cannot be explained by x_c. Strength was controlled by voids in this range. Modulus and strength cannot be directly related to f_c, since the tensile properties increased markedly with λ, where f_c remained almost constant. To obtain a greater understanding of void structures, we are currently conducting image analysis of voids.

Superheating

Figure 9 shows melting point vs. heating rate of drawn fibres with various draw ratios. The squares show the values for needle-like POM crystal reported by Iguchi[19]. The pressurized fibre with $\lambda=26$ showed large superheating as in the case of needle-like crystal and it was slightly larger than that of the conventional fibre. The melting point of the pressurized fibre extrapolated to zero heating rate was basically the same as that of the needle-like crystal.

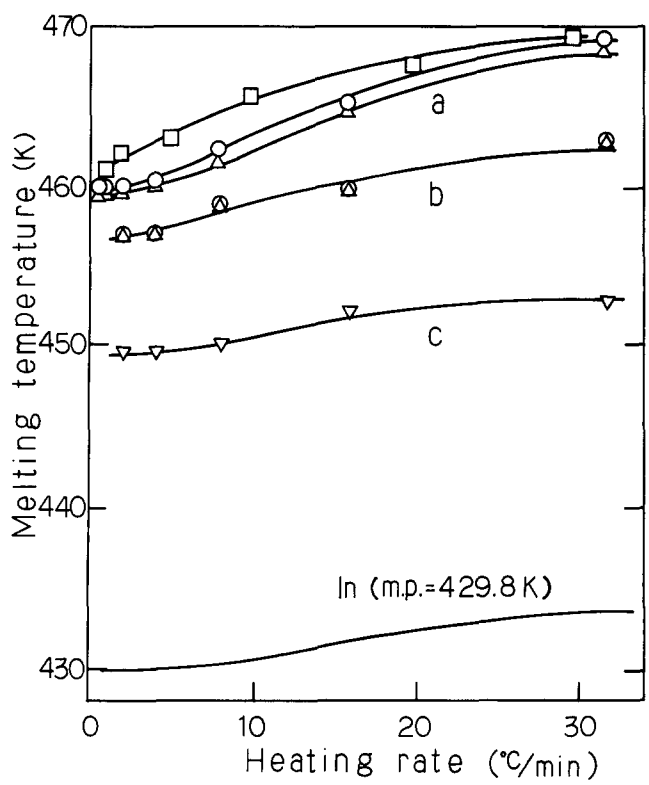

Figure 9 D.s.c. peak melting temperature vs. heating rate for drawn POM fibres: (□) POM needle-like crystal, Iguchi[19]; (○) pressurized drawn fibre; (△) conventional drawn fibre; (▽) undrawn POM; (a) $\lambda=26$, (b) $\lambda=12$, (c) $\lambda=1$

CONCLUSIONS

The superdrawn polyoxymethylene fibres produced by pressurized drawing are dense and transparent, and have good mechanical properties. The maximum apparent tensile modulus and strength and apparent density of the fibre were 53 GPa ($\lambda_{app}=31$), 2.0 GPa ($\lambda_{app}=22$) and 1.45 g cm^{-3} ($\lambda_{app}=22$), respectively. Conventional superdrawn fibres were white with maximum apparent tensile modulus and strength of 40 GPa ($\lambda_{app}=22$) and 1.4 GPa ($\lambda_{app}=18$), respectively. The improved mechanical properties are ascribed to the effect of pressure, which suppresses the generation of voids during drawing. Tensile modulus increased with x_c. Strength increased with x_c in the range of few voids, but decreased for a large number of voids in spite of increase in x_c. Strength is controlled by voids in this range. Increase in modulus and strength cannot be explained by f_c. The pressurized fibre ($\lambda=26$) exhibited pronounced superheating as noted for the needle-like crystal. The possibility of a highly chain-extended structure was indicated by analysis of a polarized Raman spectrum[22].

ACKNOWLEDGEMENTS

The authors wish to thank Professor M. Kobayashi of the Faculty of Science, Osaka University, for many useful discussions. We also would like to express our appreciation to Sofue for a solid-state n.m.r. measurement

REFERENCES

1 Asahina, M. and Enomoto, S. *J. Polym. Sci. 1932*, **54**, 1557
2 Sugeta, H. and Miyazawa, T. *Polym. J.* 1970, **1**, 226
3 Zhurkov, S. N., Levin, B. Ya. and Savitskii, A. V. *Dokl. Akad. Nauk. USSR* 1969, **186** (1), 132
4 Clark, E. S. and Scott, L. S. *Polym. Eng. Sci.* 1974, **14**, 682
5 Brew, B. and Ward, I. M. *Polymer* 1978, **19**, 1338
6 Jungniz, S., Jakeways, R. and Ward, I. M. *Polymer* 1986, **27**, 1651
7 Hope, P. S., Richardson, A and Ward, I. M. *J. Appl. Polym. Sci.* 1981, **26**, 2879
8 Coates, P. D. and Ward, I. M. *J. Polym. Sci., Polym. Phys. Edn.* 1978, **16**, 2031
9 Hope, P. S. and Ward, I. M. *Org. Coat. Plast. Chem.* 1981, **44**, 290
10 Nakagawa, K., Konaka, Y. and Yamakawa, S. *Polymer* 1985, **26**, 84
11 Takeuchi, Y., Yamamoto, F., Nakagawa, K. and Yamakawa, S. *J. Polym. Sci., Polym. Phys. Edn.* 1985, **23**, 1193
12 Konaka, T., Nakagawa, K. and Yamakawa, S. *Polymer* 1985, **26**, 462
13 Takeuchi, Y., Nakagawa, K. and Yamamoto, F. *Polymer* 1985, **26**, 1929
14 Nakagawa, K. and Konaka, T. *Polymer* 1986, **27**, 1030
15 Nakagawa, K. and Konaka, T. *Polymer* 1986, **27**, 1037
16 Nakagawa, K. and Konaka, T. *Polymer* 1986, **27**, 1553
17 Alexander, L. E. 'X-ray Diffraction Method in Polymer Science', Wiley, New York, 1969
18 Veeman, W. S., Menger, E. M., Ritchey, W. and de Boer, E. *Macromolecules* 1979, **12**, 924
19 Iguchi, M. *Makromol. Chem.* 1976, **177**, 549
20 Griffith, A. A. *Phil. Trans. R. Soc. Lond.* 1921, **221**, 163
21 Smook, J., Hamersma, W. and Pennings, A. J. *J. Mater. Sci.* 1984, **19**, 1359
22 Morishita, H., Kobayashi, M. and Komatsu, T. *Rep. Prog. Polym. Phys. Japan* 1987, **30**, 131